

PCCP

Accepted Manuscript



This is an *Accepted Manuscript*, which has been through the Royal Society of Chemistry peer review process and has been accepted for publication.

Accepted Manuscripts are published online shortly after acceptance, before technical editing, formatting and proof reading. Using this free service, authors can make their results available to the community, in citable form, before we publish the edited article. We will replace this *Accepted Manuscript* with the edited and formatted *Advance Article* as soon as it is available.

You can find more information about *Accepted Manuscripts* in the [Information for Authors](#).

Please note that technical editing may introduce minor changes to the text and/or graphics, which may alter content. The journal's standard [Terms & Conditions](#) and the [Ethical guidelines](#) still apply. In no event shall the Royal Society of Chemistry be held responsible for any errors or omissions in this *Accepted Manuscript* or any consequences arising from the use of any information it contains.

Degradation Mechanism of Sulfonated Poly(ether ether ketone) (SPEEK) Ion Exchange Membranes under the Vanadium Flow Battery Medium

Cite this: DOI: 10.1039/x0xx00000x

Received 00th January 2012,
Accepted 00th January 2012Zhizhang Yuan^{ab}, Xianfeng Li^{*a}, Jinbo Hu^c, Wanxing Xu^{ab}, Jingyu Cao^{ab}, and
Huamin Zhang^{*a}

DOI: 10.1039/x0xx00000x

www.rsc.org/

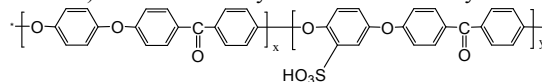
Abstract: The degradation mechanism of hydrocarbon ion exchange membranes under vanadium flow battery (VFB) medium was investigated and clarified for the first time. This work will be highly beneficial to improving the chemical stability of hydrocarbon ions exchange membranes, which is one of the most challenging issues for VFB application.

Concerns over fossil energy shortage and environmental load are the driving forces for the research efforts in renewable energies like solar and wind power. However, the intermittent and random nature of these renewable energies seriously affects the final quality of the output electricity as well as their stability in the grid. Electric energy storage (EES) becomes a valid solution to solve these problems.¹ Combined with renewable energies, energy storage can increase the quality and the stability of photovoltaic (PV) and wind-generated electricity.² As one kind of energy techniques, vanadium flow battery (VFB) has emerged as a promising alternative to existing large-scale power conversion systems due to its perfect combination of high energy efficiency, high safety and reliability.³⁻⁵ VFB, originally proposed by Maria Skyllas-Kazacos in 1985, composes of two tanks filled with active species of vanadium ions in different valance states, two pumps and a battery cell. The conversion between electricity and chemical energy is realized by reduction and oxidation of vanadium ions.^{5, 6} Although vast demonstrations of VFB in different fields have been accomplished, there still have urgent needs in developing high-quality and low-cost membranes that are believed to be vital to achieve cost effective VFB systems.⁷⁻¹⁴

Perfluorinated cation exchange membranes, such as Dupont's Nafion series^{4, 15} are the most commonly used membranes in VFB due to their superior proton conductivity and chemical stability. However, their low ion selectivity and extremely high cost have hindered their application in commercialization of VFB.² The hydrocarbon ion exchange membranes such as sulfonated polyaromatic polymers (sulfonated poly(aryl ketone ketone), poly(aryl ether sulfone), polyimide etc) are the mostly studied systems due to their tunable ions conductivity and low cost.^{12, 16} However, these membranes suffered from low chemical stability in VFB medium. The degradation mechanism of hydrocarbon ion exchange membranes has been unclear, since the medium of VFB is

very complicated (strongly acidic, oxidizing and with high electric potential). Quite recently, Hickner et al proposed a mechanism of the sulfonated poly(sulfone) (S-Radel) degradation behavior in the solution of V(V), where the reactive species first attack the S-Radel by incorporating hydroxyl groups into the polymer backbone and then oxidizing them into quinone functionalities.¹⁷ Fujimoto et al investigated the chemical stability of sulfonated Diels-Alder poly(phenylene) (SDAPP) with different ion exchange capacities (IECs), showing that the degradation was accelerated with increasing content of ion exchange groups.¹⁸ In spite of these reports, the study of degradation mechanism is very limited and the detailed degradation reaction of membranes under VFB medium is not clear, which leads to very few relevant strategies to synthesize of new materials with excellent performance for VFB application.¹⁹ Therefore, urgent need is in the clarifying degradation mechanism of sulfonated hydrocarbon membranes under VFB operating condition, which would open up a new perspective to design more durable and economically viable membranes and further accelerate VFB commercialization.

In this study, aiming at understanding the degradation of hydrocarbon ions exchange membranes, we chose sulfonated poly(ether ether ketone) (SPEEK) membranes with different DS as the model materials (Scheme 1). The influence of ions exchange group (-SO₃H) on oxidation stability during ex-situ test was investigated. To clarify the degradation mechanism, the chemical structure of the degradation products (both from ex-situ and in-situ experiments) was further analyzed and confirmed by LC/MS.



Scheme 1. The chemical structure of SPEEK

To fully understand the role of ion exchange groups on the oxidation stability of membranes, SP1 to SP3 membranes with different DS were fabricated for further investigation. The chemical structures were determined by ¹H NMR (Figure S1 of ESI†) and basic physical parameters of membranes are shown in Table 1. With DS increasing, a regular rise of water uptake and swelling rate can be observed. This can be attributed to the sulfonic acid functional groups, leading to hydrophilic water channels, which results in higher water uptake and swelling behavior.

Table 1. Physical properties of SPEEK membrane.

Membrane	Thickness(um)	DS	Water uptake (%)	Swelling (%)
SP1	100±5	0.74	49.85	20.00
SP2	100±5	0.84	67.18	25.00
SP3	100±5	0.91	70.27	27.66

To confirm the relationship between the oxidation stability and the amount of sulfonic acid functional groups, SP1, SP2 and SP3 membranes with fixed size (4 cm x 4 cm) were immersed in 0.15 M VO_2^+ to detect the concentration changes of VO_2^+ , which induced by SPEEK degradation. Obvious color change (Figure S2) has been detected in 0.15 M VO_2^+ solutions containing SPEEK membranes (40 °C) after 30 days. In contrast, the color of the solution containing SPEEK membranes turned to green as a result of reduction of VO_2^+ to VO^{2+} , which indicates that the membranes were gradually oxidized by VO_2^+ . The VO_2^+ concentration in solutions increased as DS increasing (Figure.1), suggesting that the oxidation stability of membranes decreases with the increasing DS or the sulfonic acid groups accelerated the degradation of the membrane. This possibly can be explained by the fact that the membrane with a higher DS results in higher swelling, which generates hydrophilic channels within the hydrophobic matrix. This in turn promotes the absorption of VO_2^+ and induces membrane oxidation, resulting from the contact between the polymer chains and VO_2^+ .

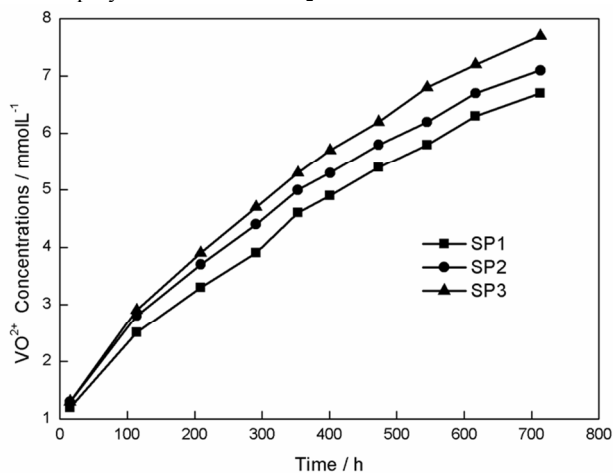


Figure 1. VO_2^+ concentration change of electrolyte solution (0.15 M VO_2^+ in 3 M total sulfate) containing SPEEK membranes at 40 °C as function of time.

To further investigate the membranes degradation mechanism, the concentration of VO_2^+ was increased to 1.5 M to accelerate the membranes degradation. After 30 h immersion, SP3 with highest DS was broken into pieces (Figure S3), while SP1 and SP2 kept intact, further confirming the role of sulfonated groups. The surface and cross section morphology of the membranes after VO_2^+ treatment was detected by SEM. All the membranes became cracked as evidenced in the surface SEM image (Figure 2) after soaking in 1.5 M VO_2^+ at 40 °C for 30 h, and the membrane becomes thinner after degradation. In addition, with DS increasing, the surface cracks became more serious, indicating that the introduction of sulfonic acid functional groups accelerated the degradation of the membrane. The cross section SEM images of original membranes and degraded membranes were detected as well (Figure 3). Compared to the original membranes, micro-pores are clearly formed (Figure 3) after soaking in 1.5 M VO_2^+ at 40 °C for 30 h. Similar to the reported results,²⁰ the SP3 membrane even suffers from grievous delaminating process where small pieces of the membrane break away from the sample (Figure 3).

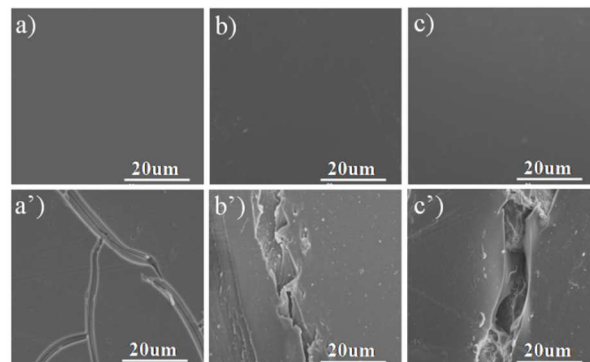


Figure 2. SEM micrographs of membrane surface: a): SP1, b): SP2, c): SP3 and after immersion in 1.5M VO_2^+ at 40 °C for 30 h: a'): SP1, b'): SP2, c'): SP3.

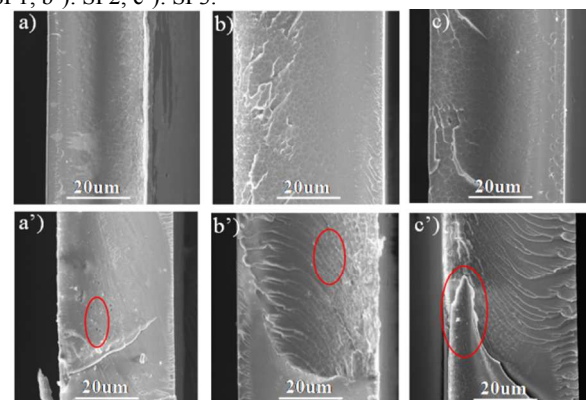


Figure 3. SEM micrographs of membrane cross-section: a): SP1, b): SP2, c): SP3 and after immersion in 1.5M VO_2^+ at 40 °C for 30 h: a'): SP1, b'): SP2, c'): SP3.

To clarify the degradation mechanism of SPEEK membranes during ex situ tests, SP3 membrane was selected as example to investigate the chemical structure of the degradation products. Figure 4 shows the ^1H NMR spectra of initial SP3 membrane (a) and SP3 membrane after immersing in 1.5 M VO_2^+ for 30 hours (b). Compared to the initial SP3 membrane, no significant differences could be found in the full ^1H NMR spectrum except for the new aromatic protons peaks emerged at around 6.9 ppm and 7.7 ppm after degradation, suggesting that no aliphatic carbon were produced during ex situ degradation. In addition to this, chemical shift and signal intensity (Figure 4) of the ortho hydrogen atoms of sulfonic acid group did not change obviously before and after degradation, suggesting that sulfonic acid functional groups remained unchanged after degradation. This conclusion is very different from the reported sulfonated polysulfone, where the sulfonate groups experienced some chemical degradation as well.²⁰

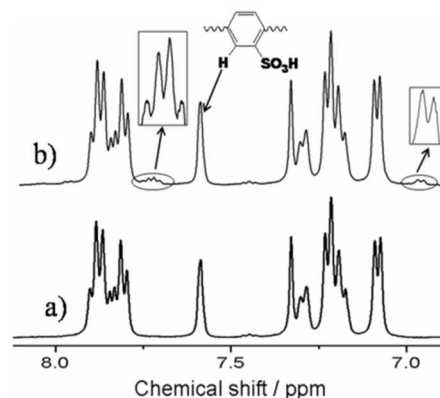


Figure 4. ^1H NMR spectra of SP3 membrane in DMSO-d_6 : a) initial; b) degraded.

FTIR was employed to confirm the chemical structure of the initial and degraded SP3 membranes. The FTIR results were displayed in Figure 5. Peaks at 1026 cm^{-1} and 1080 cm^{-1} are attributed to the asymmetric and symmetric stretching of the S=O bond from sulfonic acid functional groups for both initial (a) and degraded (b) SP3 membranes, again confirming that the sulfonic acid functional groups remained stable during ex situ degradation. The full FTIR spectra did not show obvious difference between the initial and degraded SP3 membranes, indicating again that no aliphatic carbon was formed during ex situ test.

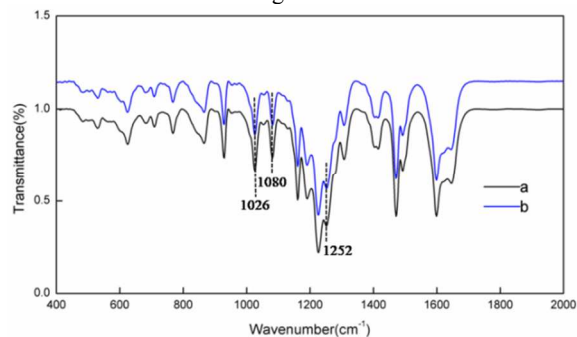


Figure 5. FTIR spectra of initial SP3 membrane (a) and degraded SP3 membrane (b).

TEM was performed on the initial SP3 and degraded SP3 membranes after staining with 1 M AgNO_3 to detect the distribution of sulfonic acid functional groups. The dark spots of initial and degraded membranes in Figure 6 (a, b) are attributed to clusters formed by the interaction between Ag^+ and negatively charged sulfonic acid groups of the membrane, indicating that sulfonic acid functional groups remained unchanged after degradation.

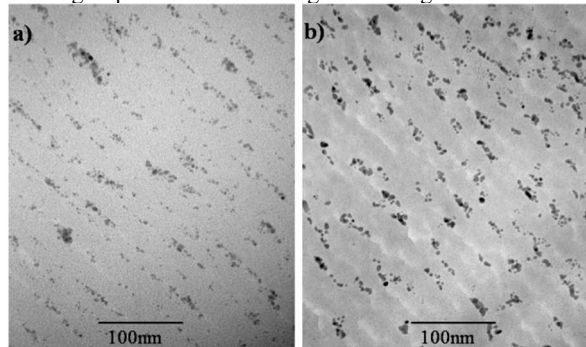
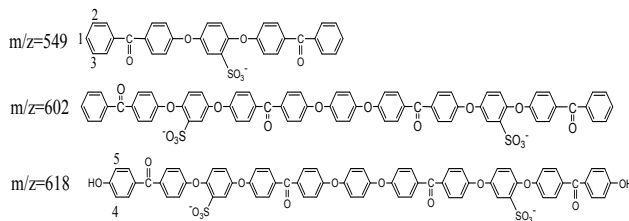


Figure 6. Distribution of $-\text{SO}_3\text{H}$ of SP3 membrane: a) initial; b) degraded.

^1H NMR and TEM results demonstrated that the polymer backbone experienced grievous chain rupture while sulfonic acid functional groups have remained stable. But the new aromatic peaks in Figure 4 b emerged at a relatively low intensity, which was very difficult to assign due to the complex random polymer. To further identify the chemical structure of degradation products, the immersing time was prolonged to 54 h to degrade the membranes into shorter chains. As expected, the SP3 membrane was broke up into small pieces after treatment. And we surprised to find that the degradation products with smaller molecular weight become water soluble (Figure S4), indicating the existence of sulfonic acid groups.

To further identify the chemical structure of the degradation products, LC/MS was employed to detect their molecular weights. The full LC/MS spectrogram of aqueous solution with negative mode is rather complicated and as shown in Figure S5. However,

some major characteristics fragment ion peaks can be recognized and identified as the structures in scheme 2.



Scheme 2. Parts of fragment ion peaks get by LC/MS.

Judging from these fragment ion peaks, we can draw a conclusion that the polymer backbone was broken from the ether bond while leaving the sulfonic acid functional groups stable. The structure of the degradation products can well explain new aromatic peaks emerged in Figure 4 b. After the ether bond cracked, new aromatic hydrogen such as H1 in scheme 2 appeared. H1, H2, H3 in scheme 2 are quad peak while H4, H5 are double peak in ^1H NMR, which can perfectly match the new peaks emerged in ^1H NMR (Figure 4) after 30 h's degradation.

^1H NMR was performed on the degraded SP3 membrane after immersion in 1.5 M VO_2^+ for 54 h for compare. Surprisingly, chemical shift and signal intensity of the new aromatic peaks in Figure 4 b have not increased so much while obvious changes have taken place on the main peaks as shown in Figure 7. This suggests again that the polymer backbone experienced grievous chain scission. Apart from this, a new peak at around 5.0 ppm is clearly emerged, which can be assigned to the complexation $-\text{OH}$, further supporting the breakage of the ether bond. There was no significant difference between the initial and the degraded SP3 membranes (soaking in 1.5 M VO_2^+ for 30 h and 54 h) in ^{13}C NMR spectra (Figure S6-S8), indicating again that no aliphatic carbon was formed during degradation.

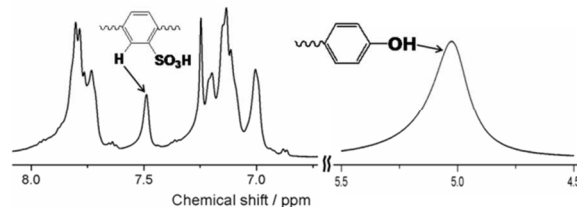
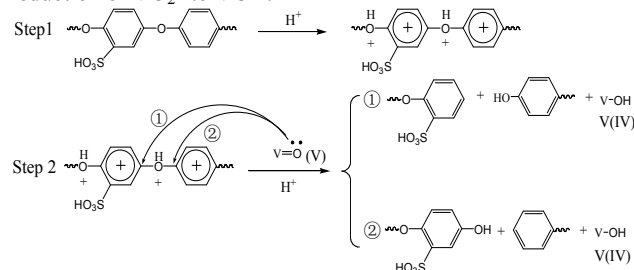


Figure 7. ^1H NMR spectra of SP3 membrane after soaking in 1.5 M VO_2^+ for 54 h.

Based on the above results, the degradation mechanism of SPEEK membrane can be proposed as shown in scheme 3. Under the strong acidic conditions, the ethereal oxygen atoms in SPEEK could be easily protonated and become strong electro-withdrawing groups. The protonated ether functionality together with the strong electron-withdrawing sulfonic acid group induce a strong electrophilic carbon center on the benzene ring, which can be easily attacked by the lone pair electron on the vanadium(V) oxygen species. According to the previous report,¹⁷ membrane soaked in the VOCl_3 exhibits no degradation during ex situ test, which can offer important information that the acidic medium greatly promoted the vanadium ion (V) oxidation. This can be explained by the theory of contrapolarization.^{21, 22} The charge at the center of the vanadium atom (V) in vanadium(V) oxygen species is very high, leading to strong polarization effect, which in turn result in deformation of the electron clouds of the oxygen, making the oxygen close to vanadium(V) electronegative. While under the strong acidic medium, H^+ was almost a naked proton, which has very strong attraction for the electron cloud, resulting from its extremely high positive charge density. The polarization of oxygen resulting from H^+ and

vanadium(V) is opposite, known as contrapolarization. The contrapolarization effect of H^+ makes the oxygen close to H^+ electronegative while the oxygen close to vanadium(V) electropositive, weakening the covalent bond between the vanadium(V) and oxygen atoms. This contrapolarization effect makes the covalent bond breaking up easily, further facilitating the reduction of VO_2^+ to VO^{2+} .



Scheme 3. The degradation mechanism of SP3 membrane during ex situ test.

To support our above supposed mechanism, SP3 membranes were immersed in 0.15 M VO_2^+ solutions with different concentration of sulfuric acid (1 M, 2 M, 3 M) to clarify the role of protonation. As evidenced in Figure 8, with increasing acid concentration, the concentration of VO_2^+ reduced from VO_2^+ increases and the degradation becomes more seriously, further confirming our assumption.

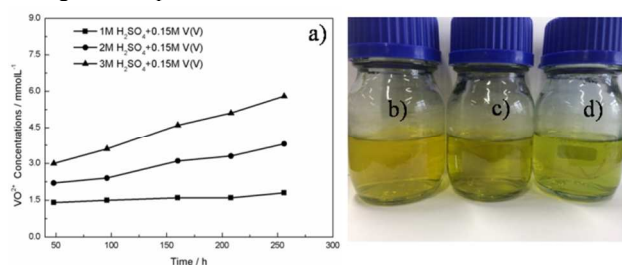


Figure 8. Influence of protonation on membrane oxidation stability: a) VO_2^+ concentration change containing SP3 membranes at 40 °C as function of time; b) SP3 membrane+1 M H_2SO_4 +0.15 M VO_2^+ ; c) SP3 membrane+2 M H_2SO_4 +0.15 M VO_2^+ ; d) SP3 membrane+3 M H_2SO_4 +0.15 M VO_2^+ .

The degradation mechanism of the above ex situ tests maybe differ from the practical degradation process in VFB since some dynamic factors are ignored, especially the high potential. Therefore, in-situ online test was carried out via single VFB cell cycling test. VFB assembled with SP3 shows CE, EE and VE of 96 %, 84 % and 88 % at current density of 80 mAcm^{-2} , which is a bit higher than commercialized Nafion115.²³ However, the performance suddenly dropped after continuously running for more than 100 cycles (Figure 9).

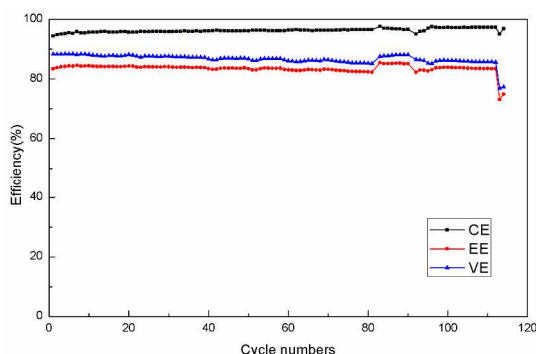


Figure 9. The on-line cycle performance of VFB assembled with SP3 membranes

SEM was employed to investigate the change of membrane morphology after lifetime test. In Figure 10 a, membrane facing the positive half cell was covered with cracks and pores, while membrane facing the negative half cell exhibited no significant changes as proofed in Figure 10 b, indicating that the VO_2^+ ions existing in positive electrolyte serve as the main sources that induce the degradation of the membrane. Figure 10 c shows the cross-section of SP3 membrane after cycle life test, inner pores are generated throughout the membrane as a result of the membrane degradation. The edge of the membrane facing the positive half cell has already crashed as marked in red line in Figure 10 c.

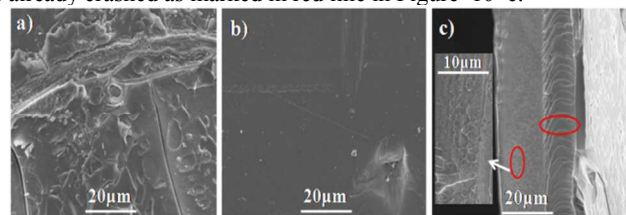


Figure 10. SEM micrographs of SP3 membrane surface after lifetime test: a) facing positive half cell; b) facing negative half cell; c) cross-section after lifetime test.

For comparison, 1H NMR study was carried out on the SP3 membrane after lifetime test as well (Figure 11). Compared with the degradation products of SP3 membrane from ex-situ test, 1H NMR spectra of SP3 membrane after lifetime test show overall the same peaks with the membranes after soaking in 1.5 M VO_2^+ for 30 h (Figure 11 a). The same new aromatic peaks are also emerged in the 1H NMR spectra after lifetime test as well. The results showed that the structure of the degradation products after cycling test is the same with that during ex situ degradation. The existence of electric field will not affect the degradation mechanism of the membranes under VFB operating condition, indicating the availability of ex-situ oxidation stability test. Even though, the chemical shift of SP3 membrane after cycling test moves to the high field as a whole as evidenced in Figure 11 b. This can be explained by the different vanadium ions existed in membranes. For ex-situ test, VO_2^+ ions are adsorbed by membranes, while, under VFB charge/discharge test, VO^{2+} ions are reported to be the most adsorbed ions in the membranes.^{24, 25} The interaction between sulfonic acid groups and different vanadium ions possibly induces the different chemical shift.

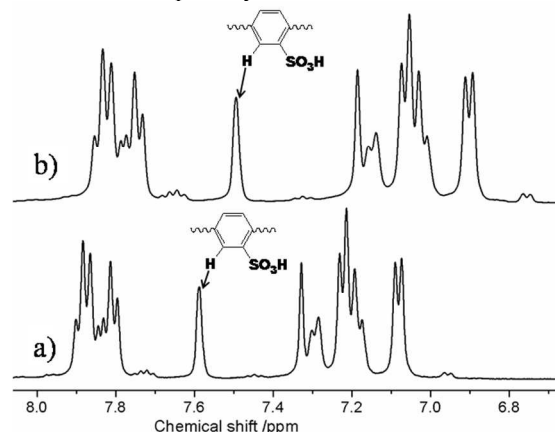


Figure 11. 1H NMR spectra of SP3 membrane: a) soaking in 1.5 M VO_2^+ for 30 h; b) after lifetime test.

Conclusions

SPEEKs with different DS were prepared and selected as model compound to investigate the degradation mechanism of hydrocarbon membranes under VFB operating condition. The degradation mechanism was proposed clearly for the first time, which was supported by experimental data. According to the proposed mechanism, apart from the sulfonic acid groups, the protonation of ether oxygen atoms under strong acid medium play very important roles in accelerating membrane degradation. Therefore, strategies such as protecting the ether bond or synthetic new compounds without ether bond or introducing electron-donating groups to aromatic backbone could be very effective to improve the oxidation stability of the membrane for VFB application.

Notes and references

Experimental part

MATERIALS AND METHODS

Materials

Poly (ether ether ketone) was kindly provided by Changchun Jilin University Special Plastic Engineering Research. 1.5 M VO₂⁺ in 3.0 M total sulfate solution was prepared by oxidation of 1.5 M VOSO₄+1.5M H₂SO₄ and the 0.15 M VO₂⁺ in 3.0 M total sulfate solution was prepared by diluting the 1.5 M VO₂⁺ in 3.0 M total sulfate solution with sulfuric acid according to literature.²⁰ All the other chemicals were used as received without further purification.

Membrane preparation

SPEEK polymers with various DS were prepared by direct sulfonation of PEEK with sulfuric acid at 40 °C for 6 h, 9 h and 10.5 h respectively, as described elsewhere.²⁶ The sulfonated degree, which was determined by ¹H NMR,²⁷ is in the range between 0.74 and 0.91 and is referred as to SP1, SP2 and SP3 respectively. The SPEEK membranes were cast from 25 wt% N, N-dimethylacetamide (DMAc) solutions and dried. Afterward, the membranes were peeled off and the thickness of membranes was 100±5 μm. To detect the water uptake and swelling of the membranes, membranes were first soaked in deionized water for 3 days in order to saturate them with water. Then the weight of the saturated membrane was obtained after quickly wiping out the surface water by tissue. The water uptake is defined as the weight ratio of the absorbed water to the dry membrane, as shown in Eq. (1):

$$\text{Wateruptak e(\%)} = \frac{W_s - W_d}{W_d} \times 100 \quad \text{Eq. (1)}$$

Where W_s and W_d are the weight of saturated and dry membrane, respectively.

While the swelling is defined as the length ratio of swollen membranes to the dry membranes, as shown in Eq. (2):

$$\text{Swelling (\%)} = \frac{L_s - L_d}{L_d} \times 100 \quad \text{Eq. (2)}$$

Where L_s and L_d are the length of saturated and dry membrane, respectively.

Ex situ oxidation stability test

To investigate the influence of ions exchange groups on the oxidation stability of membranes, SPEEK membranes with fixed size (4 cm x 4 cm) were soaked in 60 ml electrolyte solution (0.15 M VO₂⁺ in 3 M total sulfate) in sealed glass vials at 40 °C respectively. During the test, a 4ml electrolyte was collected from each vial at a regular time interval and the VO₂⁺ concentration in the electrolyte

samples was detected by UV-Vis. To better understand the degradation mechanism, SP3 with the highest DS was selected as example, more concentrated VO₂⁺ solution (1.5 M VO₂⁺ in 3 M total sulfate) was used to accelerate the membrane degradation and the degradation products were further analyzed. The immersion time was kept at 30 and 54 h respectively.

“On-line” or in-situ VFB cycle life test

For compare, the on-line cycle life test was carried out on SP3 via VFB single cell test as well. The detailed information on VFB assembly was reported previously.²⁸ A VFB single cell was assembled by sandwiching a membrane with two carbon felt electrodes, clamped by two graphite polar plates. All these components were fixed between two stainless plates. 30 ml 1.5 M VO₂⁺/VO₂⁺ in 3.0 M H₂SO₄ and 30 ml 1.5 M V²⁺/V³⁺ in 3.0M H₂SO₄ were used as positive and negative electrolytes respectively. The electrolyte was cyclically pumped through the corresponding electrodes in airtight pipelines. Charge-discharge cycling tests were conducted by ArbinBT2000 with a constant current density of 80 mA cm⁻². The cut-off voltage for discharge and charge was set at 0.8 V and 1.65 V respectively to avoid the corrosion of carbon felts and graphite polar plates. After cycle test, the composition of membrane structure was analyzed in detail.

Characterization

¹H NMR and ¹³C NMR were recorded on BRUKER DRX400 by using DMSO-d₆ as solvent and tetramethylsilane (TMS) as internal standard. UV-Vis spectrometer (JASCO, FT-IR 4100, Japan) was employed to determine the concentration of VO₂⁺. Ultra-High Definition (UHD) Accurate-Mass Q-TOF LC/MS was recorded on Agilent 6540 Q-TOF to determine the degradation products with negative mode. The instrument parameters are as follows: gas temperature: 325 °C; flow rate of drying gas: 8 L/min; Nebulizer: 25 psig; VCap: 3500 V; fragmentor: 175 V; skimmer: 65 V; OCT: 1 RF; Vpp: 750 V; Mass range: 50-1700. The distribution of negatively charged groups (-SO₃H) in the membrane samples before and after degradation were recorded by TEM (JEM-2000EX, JEOL). All the prepared membrane samples were dyed with 1M silver nitrate solution and then washed with deionized water to remove the silver ions absorbed in the membrane. After that, the membranes were dried and then fixed in epoxy before being cut into thin slice samples. Fourier transformed infrared spectroscopy (FTIR) (Avatar.370 E.S.P., Nicolet Continuum Infrared Microscope) was used to determine the chemical structure of the membranes before and after degradation. The membrane samples were first dissolved in DMAc to form a 4 wt% solution and then cast onto a KBr crystal. The KBr crystal was then dried at 60 °C under ambient pressure for 12 h, followed by drying under vacuum for 24 h at 80 °C. The cross-section and surface morphologies were detected by SEM (JEOL 6360LV, Japan) with an acceleration voltage of 10 kV. The cross-sections were obtained by breaking the membranes in liquid nitrogen and coating them with gold prior to imaging.

^a Division of energy storage, Dalian Institute of Chemical Physics, Chinese Academy of Sciences, Zhongshan Road 457, Dalian 116023, China, Email: lixianfeng@dicp.ac.cn, zhanghm@dicp.ac.cn

^b University of Chinese Academy of Sciences, Beijing 100039, China

^c Key Laboratory of Organofluorine Chemistry, Shanghai Institute of Organic Chemistry, Chinese Academy of Sciences, 345 Ling-Ling Road, Shanghai, 200032 (China)

†Electronic Supplementary Information (ESI) available: Experimental section; NMR, FTIR, SEM, LC/MS spectra; fragment ion peaks. See DOI: 10.1039/c000000x/

1. Bruce Dunn, Haresh Kamath and J.-M. Tarascon, *Science*, 2011, **334**, 928-935.
2. X. Li, H. Zhang, Z. Mai, H. Zhang and I. Vankelecom, *Energy Environ.Sci.*, 2011, **4**, 1147.
3. H. Zhang, H. Zhang, X. Li, Z. Mai and J. Zhang, *Energy Environ.Sci.*, 2011, **4**, 1676.
4. M. Skyllas-Kazacos, M. Chakrabarti, S. Hajimolana, F. Mjalli and M. Saleem, *J. Electrochem. Soc.*, 2011, **158**, R55-R79.
5. M. Skyllas-Kazacos, M. Rychcik, R. G. Robins, A. Fane and M. Green, *J. Electrochem. Soc.*, 1986, **133**, 1057.
6. C. Ponce de León, A. Frías-Ferrer, J. González-García, D. A. Szánto and F. C. Walsh, *J.Power Sources*, 2006, **160**, 716-732.
7. T. Sukkar and M. Skyllas-Kazacos, *J.Membr.Sci.*, 2003, **222**, 249-264.
8. Q. Luo, H. Zhang, J. Chen, P. Qian and Y. Zhai, *J.Membr.Sci.*, 2008, **311**, 98-103.
9. Q. Luo, H. Zhang, J. Chen, D. You, C. Sun and Y. Zhang, *J.Membr.Sci.*, 2008, **325**, 553-558.
10. X. Teng, Y. Zhao, J. Xi, Z. Wu, X. Qiu and L. Chen, *J.Power Sources*, 2009, **189**, 1240-1246.
11. C. Jia, J. Liu and C. Yan, *J.Power Sources*, 2010, **195**, 4380-4383.
12. C. Sun, J. Chen, H. Zhang, X. Han and Q. Luo, *J.Power Sources*, 2010, **195**, 890-897.
13. B. Schwenzer, J. Zhang, S. Kim, L. Li, J. Liu and Z. Yang, *ChemSusChem*, 2011, **4**, 1388-1406.
14. W. Wang, Q. Luo, B. Li, X. Wei, L. Li and Z. Yang, *Adv.Funct.Mater.*, 2013, **23**, 970-986.
15. P. Zhao, H. Zhang, H. Zhou, J. Chen, S. Gao and B. Yi, *J.Power Sources*, 2006, **162**, 1416-1420.
16. D. Chen, S. Wang, M. Xiao and Y. Meng, *Energy Environ.Sci.*, 2010, **3**, 622.
17. D. Chen and M. A. Hickner, *Phys.Chem.Chem.Phys.*, 2013, **15**, 11299.
18. C. Fujimoto, S. Kim, R. Stains, X. Wei, L. Li and Z. G. Yang, *Electrochem.Comm.*, 2012, **20**, 48-51.
19. T. H. Yu, Y. Sha, W.-G. Liu, B. V. Merinov, P. Shirvanian and W. A. Goddard, *J.Am.Chem.Soc.*, 2011, **133**, 19857-19863.
20. S. Kim, T. B. Tighe, B. Schwenzer, J. Yan, J. Zhang, J. Liu, Z. Yang and M. A. Hickner, *J.Appl.Electrochem.*, 2011, **41**, 1201-1213.
21. K. Grjotheim, F. Grönvold and J. Krogh-Moe, *J.Am.Chem.Soc.*, 1955, **77**, 5824-5827.
22. T. L. Ho, *Res.Chem.Intermed.*, 1989, **11**, 157-224.
23. Z. Mai, H. Zhang, H. Zhang, W. Xu, W. Wei, H. Na and X. Li, *ChemSusChem*, 2013, **6**, 328-335.
24. M. Vijayakumar, M. S. Bhuvaneswari, P. Nachimuthu, B. Schwenzer, S. Kim, Z. Yang, J. Liu, G. L. Graff, S. Thevuthasan and J. Hu, *J.Membr.Sci.*, 2011, **366**, 325-334.
25. J. S. Lawton, D. S. Aaron, Z. Tang and T. A. Zawodzinski, *J.Membr.Sci.*, 2013, **428**, 38-45.
26. S. J. Zaidi, S. Mikhailenko, G. Robertson, M. Guiver and S. Kaliaguine, *J.Membr.Sci.*, 2000, **173**, 17-34.
27. G. P. Robertson, S. D. Mikhailenko, K. Wang, P. Xing, M. D. Guiver and S. Kaliaguine, *J.Membr.Sci.*, 2003, **219**, 113-121.
28. Z. Mai, H. Zhang, X. Li, C. Bi and H. Dai, *J.Power Sources*, 2011, **196**, 482-487.